

## Freezing and glass transition of hard spheres in cavities

Z. T. Németh<sup>1,2</sup> and H. Löwen<sup>1,3</sup>

<sup>1</sup>*Institut für Festkörperforschung, Forschungszentrum Jülich GmbH, D-52425 Jülich, Germany*

<sup>2</sup>*Veszprémi Egyetem, Fizika Tanszék, Egyetem ut 10, H-8200 Veszprém, Hungary*

<sup>3</sup>*Institut für Theoretische Physik II, Heinrich-Heine-Universität Düsseldorf, Universitätsstraße 1, D-40225 Düsseldorf, Germany*

(Received 3 September 1998)

Dynamical and static properties of  $N=13-4000$  hard spheres in spherical cavities with smooth and rough walls have been calculated by molecular-dynamics computer simulations. We use a dynamical criterion to distinguish between fluidlike and solidlike states. The associated crossover densities show a strong dependence both on the system size and on the surface roughness. For large  $N$ , these crossover densities tend to the *bulk glass transition* density for rough walls and to the *bulk crystallization* density for smooth walls. The crossover densities for finite  $N$  are found to be significantly smaller than the corresponding bulk densities. A detailed examination of the layer-resolved radial- and tangential mean-square displacements reveals qualitatively different dynamics for smooth and rough cavities. [S1063-651X(99)00105-1]

PACS number(s): 64.70.-p, 61.20.Ja

### I. INTRODUCTION

The dynamics of confined systems can be drastically different from the corresponding bulk behavior [1]. An intriguing question concerns the microscopic mechanisms which induce such changes. A large number of different experimental works on the kinetic glass transition in confined systems [1–5] has been published during the past decade, however a general microscopic background is still missing. The measurement of dynamical features of complicated organic molecules (salol, pentylene glycol, propylene glycol, etc.) in porous materials is, however, confronted with serious difficulties, such as the dubious determination of the density within the pores, the lack of knowledge of effective interparticle and particle-wall interactions, etc., which do play an important role during the transition process. The experimental results are sometimes inconclusive even regarding elementary questions such as, for example, the shift of the glass transition temperature compared to the bulk [3]. For technical applications as well as from a more fundamental point of view, it is necessary to understand in detail how the structural, dynamical, and rheological properties are affected by the interparticle- and particle-wall interactions. In particular, a molecular roughness of the walls is expected to slow down the dynamics near the walls. This was recently demonstrated in experiments on van der Waals glasses in nanopores with and without lubricated surfaces [4].

In this paper we study this effect theoretically within a model of hard spheres confined in spherical cavities. The model is simple since the interactions are governed only by packing effects. For the wall-particle interaction, we also assume an excluded volume form. However, we include surface roughness explicitly. This enables us to compare the dynamics directly with that in a smooth cavity. The model can be realized for spherical molecules confined to spherical pores [5]. A possible realization of our simple model can be colloidal particles confined in water droplets or vesicles, where besides the accurate knowledge of the density and the shape of the confining geometry, the direct optical observation of the particle dynamics would be possible as well [6].

Previous work has focused on three related but complementary aspects: First, *planar* walls were considered; particular attention was paid to the precrystallization transition of hard spheres near hard smooth walls [7,8] and to phase transitions in hard-sphere fluids confined between two parallel smooth walls [9]. Furthermore, a periodic structure on top of a planar wall was studied, see, e.g., [10]. In particular, the structural properties of grooves consisting of a periodic array of saw-toothed wedges was recently investigated by computer simulation [11] and density-functional theory [12]. Also the effect of surface roughness was recently considered for a planar geometry [13]. In this work we extend such studies to a random wall roughness and a curved surface. As a second aspect of previous work, the thermodynamics in different ensembles and density profiles were investigated within our model for smooth curved walls [15–17]. In our paper we focus more on the single-particle dynamics of the system and include a possible wall roughness as well. Finally, the glass transitions [18] and the freezing transition [19] in clusters were recently studied. These clusters are finite but structurally different from confined fluids.

Our main result is that the dynamics and the location of the freezing transition depend crucially on the wall roughness and on the finite size of the confined system. The wall roughness may even trigger the overall dynamics of a large system by preventing crystallization near the walls and forcing the hard spheres into a glassy structure [20,21].

The paper is organized as follows. In Sec. II we introduce our model. Then in Sec. III we focus on structural properties. The major part of this paper concerns the dynamics measured by the mean-square displacements of the individual particles. In particular, we discuss the distance-resolved dynamics for smooth and rough walls in Sec. IV. Finally, Sec. V is devoted to a discussion and an outlook.

### II. THE MODEL

We have performed molecular-dynamics simulations for hard spheres (HS) confined in spherical cavities. Both smooth and rough cavity walls were investigated. Our model

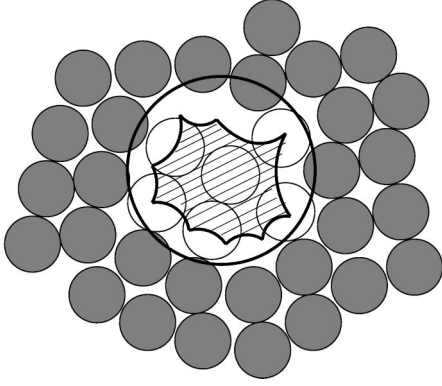


FIG. 1. Schematic picture of a cavity with a rough wall. The white spheres represent the mobile particles, the fixed dark particles constitute the rough cavity wall.

system contained  $N=13-4000$  hard spheres of diameter  $\sigma$  interacting via the pair potential

$$V_{\text{HS}}(r) = \begin{cases} 0, & r > \sigma \\ \infty, & r \leq \sigma, \end{cases} \quad (2.1)$$

where  $r$  is the interparticle distance of the particles. Henceforth, the particle positions are denoted by  $\vec{r}_i$ , where  $i = 1, \dots, N$ .

In the case of a smooth wall, the spheres interact with the cavity wall via an external potential. For a sphere at position  $\vec{r}$ , the potential energy is

$$V^{\text{ext}}(\vec{r}) = \begin{cases} 0, & r \leq R - \sigma/2 \\ \infty, & r > R - \sigma/2, \end{cases} \quad (2.2)$$

where  $R$  stands for the cavity radius and  $r = |\vec{r}|$  is the distance of the particle from the origin of the coordinate frame, which is taken to be the cavity center.

Cavities with rough walls have been built from  $N_f$  fixed ‘‘boundary’’ hard spheres of the same diameter  $\sigma$ , see Fig. 1. Details of this procedure are described later. In this case, the external potential can be written as

$$V^{\text{ext}}(\vec{r}) = \sum_{i=1}^{N_f} V_{\text{HS}}(\vec{r} - \vec{r}_i^{(f)}), \quad (2.3)$$

where the  $\vec{r}_i^{(f)}$  ( $i = 1, \dots, N_f$ ) denote the position of the fixed wall particles.

Due to the excluded volume interactions in our model, the temperature  $T$  only sets the relevant energy scale  $k_B T$ , thus the single remaining thermodynamic parameter is the number density per unit volume,  $\rho = N/V$ , or the corresponding *packing fraction* defined by

$$\eta = N \pi \frac{\sigma^3}{6V}. \quad (2.4)$$

Here  $V$  is the physical volume which can be covered by the spheres inside the cavity. Of course, this volume is in general larger than the free volume which can be accessed by the center-of-mass coordinates of the free particles. For spherical

cavities with smooth walls, clearly  $\eta = N(\sigma/8R)^3$ , while we determine  $V$  and  $\eta$  for each rough wall by a Monte Carlo calculation.

We have studied the above models by a molecular-dynamics computer simulation for several  $N$  at various densities. Cavities with rough walls were constructed as follows: we generated a random packing (RP) configuration of 729 HS with a packing fraction of  $\eta = 0.61$  applying the efficient algorithm of Jodrey and Tory [23]. The periodic boundary conditions allowed us to use this block as a ‘‘brick’’ and build larger blocks containing many thousands of particles. Hereupon we marked a spherical cluster inside the block, around an arbitrarily chosen particle whose position served from this point on as the center of the cavity. The cluster was ‘‘spherical’’ in the sense that those  $N$  particles were chosen which were inside a spherical shell around the central one. After this, we scaled the diameters of every particle to enable the change of positions of the members of the marked cluster, but not allowing the escape through the wall consisting of the surrounding unmarked particles. As already stated, the volume  $V$  which we need to fix the packing fraction was measured by Monte Carlo simulation with a relative accuracy of about  $10^{-2} - 10^{-3}$ .

In the case of smooth walls, the spherical symmetry allows trivial overall rotation of the whole system around the cavity center. As a consequence of the conservation of the total angular momentum of hard spheres in our model, this global rotation would survive in the simulation, precluding the observation of the interesting part of the dynamics. To avoid this, we set the total angular momentum of the hard spheres to be zero in all of our future considerations and simulations.

A simulation cycle started with an equilibration period of typically  $10^3 - 10^4$  collisions per particle followed by a production run of  $10^4 - 10^5$  collisions per particle. In the case of rough walls, we have averaged data from 10–30 simulation cycles performed for different cavities at the same packing values  $\eta$ .

### III. STRUCTURAL PROPERTIES

First we have calculated the radial density profile  $\rho(r)$  defined as

$$\rho(r) = \left\langle \frac{1}{4\pi r^2} \sum_{i=1}^N \delta(r - \vec{r}_i) \right\rangle, \quad (3.1)$$

where  $\langle \dots \rangle$  denotes a static canonical average of the finite system:

$$\begin{aligned} \langle \dots \rangle &= \frac{1}{Z_N} \int d\vec{r}_1 \dots \int d\vec{r}_N \dots \left( \prod_{i < j=1}^N \Theta(|\vec{r}_i - \vec{r}_j| - \sigma) \right) \\ &\times \left( \prod_{n=1}^N \exp[-V^{\text{ext}}(\vec{r}_n)] \right). \end{aligned} \quad (3.2)$$

Here the prefactor  $Z_N$  ensures correct normalization ( $\langle 1 \rangle = 1$ ) and  $\Theta(x)$  denotes the unit step function. The *radial* probability density to find one particle at a distance  $r$  from the origin is given by  $4\pi r^2 \rho(r)$ . The contact value of  $\rho(r)$  for smooth walls was determined via

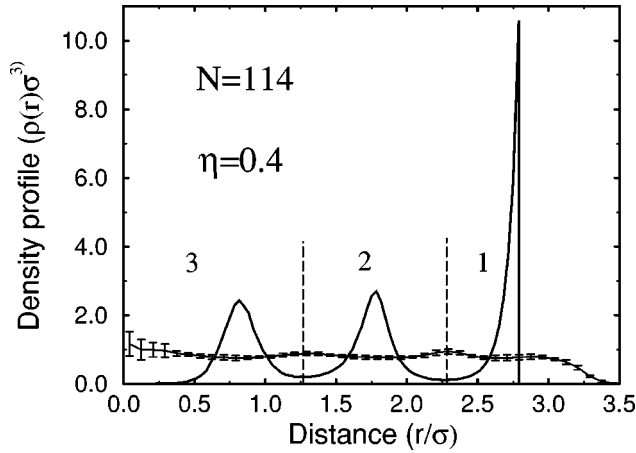


FIG. 2. Radial density profile  $\rho(r)\sigma^3$  versus reduced distance  $r/\sigma$  for  $N=114$  hard spheres in spherical cavities with smooth (solid line) and rough walls (curve with bars). The different shells labeled by the numbers 1, 2, and 3 are indicated by the vertical dashed lines. The curve with bars is an averaged density profile for 10 different rough cavities having the same value of the packing fraction as in the smooth case ( $\eta=0.4$ ). The bars show the standard deviation of the densities from their mean value.

$$\rho\left(R - \frac{\sigma}{2}\right) = P_w/k_B T, \quad (3.3)$$

where  $P_w$  is the wall pressure which can be directly measured as a time average of the particle-wall collisions [24].

Results for  $N=114$  are given in Fig. 2. As expected, the density profile is strongly inhomogeneous in the smooth case (solid line), exhibiting several peaks in accordance with the layering of particles in concentric spherical shells around the cavity center. We have labeled the different shells by integers and fixed the width of the shells by the minima of the density profile, see Fig. 2. The smoother curve in Fig. 2 represents  $\rho(r)$  averaged for 10 different cavities of rough walls each with the same packing fraction  $\eta=0.4$ . The bars show the standard deviation of the data. As expected, the structure is drastically smeared out since the rough wall induces disorder exactly on the length scale of the spheres. Of course, due to our construction of the rough cavities where a central particle exists at the origin, there is a slight increase of the density profile at the origin. Finally, we remark that the structure of similar systems has been studied by other authors as well [14–17], but only cavities with smooth walls were discussed.

#### IV. DYNAMICAL FEATURES

Let us now explore dynamical features which provide a sensitive diagnostics in locating freezing and glass transitions. We have measured the averaged root-mean-square displacement  $\Delta$  after  $N_c$  collisions per particle which is defined as

$$\Delta(N_c) = \left( \frac{1}{N} \left\langle \sum_{i=1}^N |\vec{r}_i(0) - \vec{r}_i(t_c)|^2 \right\rangle \right)^{1/2}. \quad (4.1)$$

Here  $\vec{r}_i(t)$  denotes the time-dependent trajectory of the  $i$ th particle and  $t_c$  is the time after  $N_c$  collisions per particle.

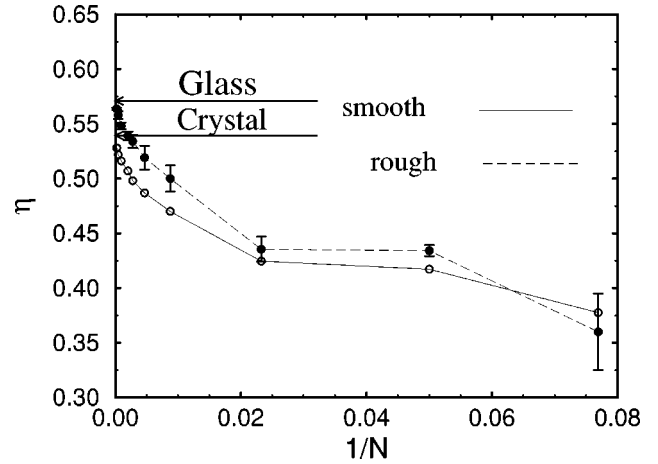


FIG. 3. Crossover packing fractions  $\eta_c$  versus  $1/N$  for smooth walls (open circles) and rough walls (full circles). Data are given for  $N=13, 21, 43, 114, 214, 360, 496, 1048, 2093,$  and  $4000$ . For smooth walls the statistical errors are smaller than the symbol size; in the case of rough walls the bars show the standard deviation of the transition packing fractions obtained from different rough cavities. The lines between the symbols are a guide to the eye. The packing fractions of the bulk freezing and glass transition are indicated by arrows.

This quantity clearly characterizes the mobility of particles. In bulk systems,  $\Delta(N_c)$  will diverge as  $N_c \rightarrow \infty$  due to a finite long-time diffusion; in a finite system, however,  $\Delta(N_c)$  stays finite. The root-mean-square displacement  $\Delta$  has proven to be a key quantity in investigating freezing and glass transition in bulk fluids. For fixed  $N_c$ ,  $\Delta$  varies slowly as a function of the thermodynamic parameters in the fluid phase, whereas it drops rapidly to smaller values as the system arrives at a freezing or glass transition regime [25,28]. In our molecular-dynamics simulations, we have measured  $\Delta$  for smooth and rough cavities containing  $N=13-4000$  particles and we have looked for drastic dynamical changes as functions of the packing fraction. Throughout our calculations,  $N_c$  was fixed to be 500. We used the following dynamical criterion to locate the freezing or glass transition: If  $\Delta$  is  $\sigma/2$  after  $N_c \equiv 500$  collisions per particle, then the associated packing fraction is called *crossover packing fraction*  $\eta_c$ . Although this criterion seems to be arbitrary at first glance, it has a number of advantages: First, it will perfectly reproduce the *bulk* freezing and glass transition of hard spheres. Second, it is easy to implement and to handle. Third, it fixes the crossover packing fraction with excellent accuracy since  $\Delta$  depends sensitively on the density change.

Results for the crossover packing fractions  $\eta_c$  as a function of the inverse total number of mobile spheres  $1/N$  are given in Fig. 3. The bulk case can directly be obtained by taking the limit  $1/N \rightarrow 0$ . In order to facilitate comparison between smooth- and rough walls, we have chosen the same numbers of particles in both cases, namely  $N=13, 21, 43, 114, 214, 360, 496, 1048, 2093,$  and  $4000$ . For rough walls the bars indicate the standard deviation of the data from their mean values; for smooth walls the statistical error is smaller than the symbol size. As a result, the crossover packings *decrease* with decreasing system size, similar to a two-dimensional system of a hard disk in spherical cavities [22]. This means that, for fixed density, the dynamics is slower in

a finite system as compared to the bulk.

As is also clearly visible from Fig. 3, the crossover packing fractions strongly differ for systems having the same  $N$  number of particles but different surface roughness. Interestingly enough, this difference becomes more pronounced with increasing system size. For large  $N$  and rough walls, the crossover packing fraction tends to a value near the *bulk glass transition* which occurs at  $\eta_g \approx 0.57 \pm 0.01$  [26,25,28]. On the other hand, for smooth walls, the crossover packing fractions tend to the bulk freezing transition [27]. The reason for that can be understood as follows: For smooth walls the system precrystallizes near the walls [7]. Hence the crystalline order is induced by the walls and proceeds into the cavity leading directly to a crossover at the bulk freezing transition as  $N \rightarrow \infty$ . On the other hand, a rough disordered wall composed of fixed spheres favors a glassy surrounding and induces a glassy layer on top of the walls. Consequently the dynamical crossover happens close to the bulk glass transition density. Of course, for extremely large systems, again bulk crystallization will dominate and force the system to reach the bulk freezing density as  $N \rightarrow \infty$ . Let us also briefly comment on very small systems  $N=13$  where the dynamics in rough cavities seems to be slightly slower than that in smooth cavities: This is due to a local blocking of particle displacements by the rough walls.

We have finally calculated the radial and the tangential dynamics resolving the latter in different spherical shells. First, we define the radial component of the root-mean-square displacement via

$$\Delta_R(N_c) = \left( \frac{1}{N} \left\langle \sum_{i=1}^N [|\vec{r}_i(0)| - |\vec{r}_i(N_c)|]^2 \right\rangle \right)^{1/2}. \quad (4.2)$$

Similarly we introduce a shell-resolved tangential component of the root-mean-square displacement. In order to do so, we characterize the different shells by starting from the density profile of a smooth wall, see Fig. 2. This profile has  $N_m$  minima at radii  $r_m^{(k)}$  numbered from the wall to the cavity center,  $k=1,2,3,\dots$ . Particularly, we fix the outermost minimum at  $r_m^{(1)} \equiv R - \sigma/2$  and we define the inner minimum at the origin,  $r_m^{(N_m)} \equiv 0$ . Correspondingly the  $k$ th shell is bounded by the inner radius  $r_m^{(k)}$  and the outer radius  $r_m^{(k-1)}$ . The mean radius  $R_k$  of the  $k$ th shell is  $R_k = (r_m^{(k)} + r_m^{(k-1)})/2$ .

Now the tangential component of the root-mean-square displacement in the  $k$ th shell is

$$\Delta_T^{(k)}(N_c) = \left( \frac{1}{N_s^{(k)}} \left\langle \sum_{i=1}^{N_s^{(k)}} (\alpha_i R_k)^2 \right\rangle \right)^{1/2}, \quad (4.3)$$

where  $\alpha_i = \arccos\{\vec{r}_i(0) \cdot \vec{r}_i(t_c) / [|\vec{r}_i(0)| \cdot |\vec{r}_i(t_c)|]\}$  denotes the angle between  $\vec{r}_i(0)$  and  $\vec{r}_i(t_c)$  and the sum runs over all trajectories which start and end in the  $k$ th shell at  $t=0$  and  $t=t_c$ , respectively.  $N_s^{(k)}$  stands for the number of such trajectories in the  $k$ th shell. The shell resolution is identically performed for rough walls in order to facilitate a direct comparison.

Results for  $\Delta_R$  as a function of  $\eta$  are shown in Fig. 4(a). The difference between smooth and rough walls is striking: for rough walls the radial mobility is significantly higher

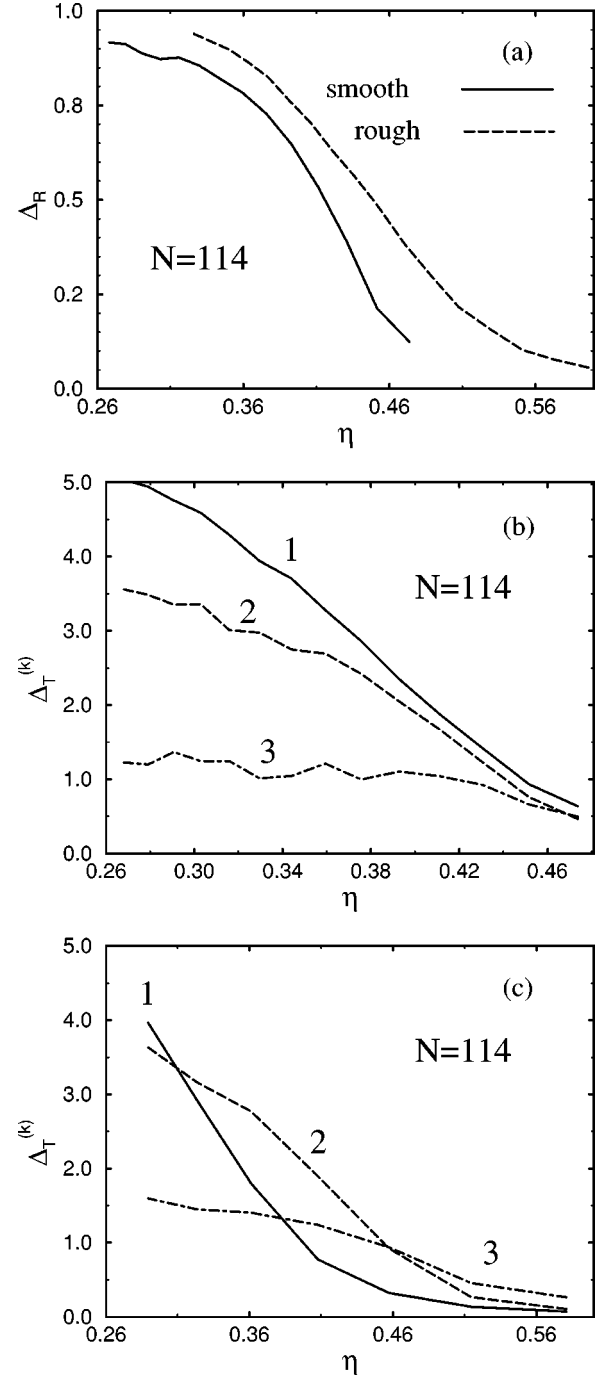


FIG. 4. (a) Averaged radial root-mean-square displacement  $\Delta_R$  versus packing fraction  $\eta$  of  $N=114$  particles for smooth (solid line) and rough (dashed line) cavities. (b) Same as (a) but now for the tangential mean-square displacements  $\Delta_T^{(k)}$  for a smooth wall. From left to right:  $k=1$  (solid line),  $k=2$  (dashed line), and  $k=3$  (dot-dashed line). (c) Same as (b) but now for a rough wall.

than that for smooth walls. This is due to the strong radial ordering in the smooth case which hinders interlayer hopping processes. On the other hand, the surface roughness destroys this ordering completely (see Fig. 2) which leads to a large radial mobility even at higher densities. Data for the shell-resolved tangential mobility  $\Delta_T^{(k)}$  are given in Figs. 4(b) and 4(c) for smooth and rough walls, respectively. In both cases, a significant heterogeneity of the dynamics induced by the observed structural ordering is observed. For smooth walls,

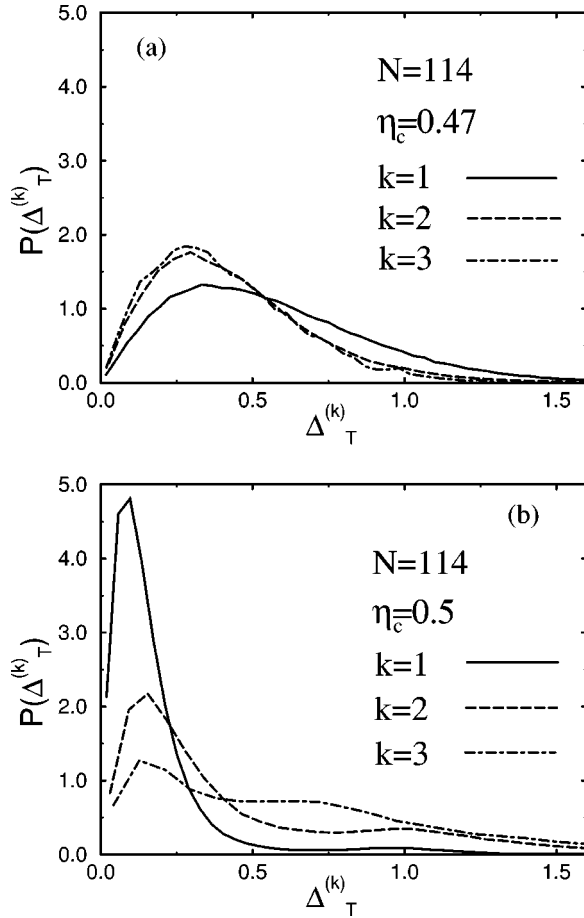


FIG. 5. (a) Probability distribution  $P(\Delta_T^{(k)})$  of the tangential mean-square displacements for  $N=114$  particles in smooth cavities at the crossover density  $\eta_c=0.47$ . (b) Same as (a) but now for rough walls at the crossover density  $\eta_c=0.50$ .

the results are as expected: the tangential mobility is highest in the outermost shell and decreases for the inner shells. Clearly,  $\Delta_T^{(1)} > \Delta_T^{(2)} > \Delta_T^{(3)}$  holds over a broad density regime up to the crossover packing fraction. This is due to fluctuations in the total angular momentum which are most pronounced in the outer shells. In the rough case, however, the picture is completely different: The above relation holds only for packing fractions up to  $\eta=0.3$ . Then the surface roughness blocks the tangential dynamics near the wall and the second layer becomes more mobile. For high densities, the above relation is completely inverted: Now the dynamics in the inner shell is less hindered by the roughness. Comparing Figs. 4(b) and 4(c) for fixed density, the tangential dynamics of the smooth case are faster than that in the rough case. However, the global dynamics dominated by the radial part are still faster in the rough case, as manifested in a higher crossover packing fraction in this case, see Fig. 3.

Figure 5 shows the probability density distribution  $P(\Delta_T^{(k)})$  of the tangential root-mean-square displacements in the three shells for smooth (a) and for rough (b) walls at the crossover packings. As can be deduced from Fig. 5(a), the

mean of the solid curve (denoting the first shell) is clearly larger than in the case of the two other shells, which have practically the same height and shape. This is consistent with our data given in Fig. 4(b). For rough walls, on the other hand, the outermost shell is slowest. There are additional maxima in the distribution at higher distances  $\Delta_T^k \approx \sigma$  indicating tangential particle hopping processes near the crossover. Such additional maxima frequently occur near the kinetic glass transition [25,28] and again support our picture that the surface roughness induces a glassy structure near the walls.

## V. CONCLUSIONS

In conclusion, we have demonstrated that the dynamics in cavities depends sensitively on the surface roughness. A cavity wall which is smooth on the typical length scale of the particles induces a strong layering and prefers, at least in our hard-sphere model, a crystalline layer. Therefore the dynamics becomes slow close to the bulk crystallization density. On the other hand, a disordered rough cavity wall prevents crystallization and prefers a glassy layer. Therefore the dynamics are faster for the rough case than for the smooth case.

As far as a comparison with actual experiments in pores [4] is concerned, several caveats are in order. First, our model system of hard spheres exhibits a freezing transition at densities which are smaller than the glass-transition density. For real molecules this may be quite different. Also we kept the total angular momentum to zero here. Such zero modes can become actually important in real smooth cavities and may accelerate the dynamics considerably for smooth cavities. Also attractive wall-particle forces may become relevant in real systems. The best realization of our model will be for colloids [29,30] confined in structured cavities. Here, however, one should bear in mind that the colloidal dynamics are Brownian rather than Newtonian as studied in this work. However, since we kept the total angular momentum to zero and the long-time dynamics is similar near the glass transition [31], the results are expected to be qualitatively similar.

We finish with a couple of remarks: First, it would be useful to explore the density profiles of rough cavities using, e.g., density-functional methods which incorporate the correct packing geometries [32]. Second, one should study more systematically the wetting behavior of structured surfaces by crystalline and glassy layers for different kinds of roughness. In the present paper we have only studied one particular kind of roughness whose length scale was comparable with that of the particles. More general studies including different topographically and energetically caused roughnesses are important to understand the dynamics of confined fluids and the microscopic nature of friction.

## ACKNOWLEDGMENT

We thank the Deutsche Forschungsgemeinschaft for their support within the Schwerpunkt ‘‘Benetzung und Struktur- bildung an Grenzflachen.’’

- [1] See, e.g., *Molecular Dynamics in Restricted Geometries*, edited by J. Klafter and J. M. Drake (Wiley, New York, 1989), and references therein.
- [2] J. Schueller *et al.*, Phys. Rev. B **52**, 15 232 (1995); P. Pissis *et al.*, J. Phys.: Condens. Matter **6**, L325 (1994); A. Schoenhals and R. Stauga, J. Chem. Phys. **108**, 5130 (1998); C. L. Jackson and G. B. McKenna, J. Non-Cryst. Solids **131-133**, 221 (1991).
- [3] Yu. B. Meln'ichenko *et al.*, J. Chem. Phys. **103**, 2016 (1995).
- [4] M. Arndt, R. Stannarius, H. Groothues, E. Hempel, and F. Kremer, Phys. Rev. Lett. **79**, 2077 (1997); M. Arndt, R. Stannarius, W. Gorbatschow, and F. Kremer, Phys. Rev. E **54**, 5377 (1996); W. Gorbatschow, M. Arndt, R. Stannarius, and F. Kremer, Europhys. Lett. **35**, 719 (1996).
- [5] G. Barut, P. Pissis, R. Pelster, and G. Nimtz, Phys. Rev. Lett. **80**, 3543 (1998).
- [6] A. D. Dinsmore, D. T. Wong, P. Nelson, and A. G. Yodh, Phys. Rev. Lett. **80**, 409 (1998).
- [7] D. J. Courtemanche and F. van Swol, Phys. Rev. Lett. **69**, 2078 (1992).
- [8] R. Ohnesorge, H. Löwen, and H. Wagner, Phys. Rev. E **50**, 4801 (1994).
- [9] M. Schmidt and H. Löwen, Phys. Rev. Lett. **76**, 4552 (1996); Phys. Rev. E **55**, 7228 (1997).
- [10] D. J. Diestler, M. Schoen, J. E. Curry, and J. H. Cushman, J. Chem. Phys. **100**, 9140 (1994).
- [11] M. Schoen and S. Dietrich, Phys. Rev. E **56**, 499 (1997).
- [12] D. Henderson, S. Sokolowski, and D. Wasan, Phys. Rev. E **57**, 5539 (1998).
- [13] L. J. D. Frink and F. van Swol, J. Chem. Phys. **108**, 5588 (1998).
- [14] Y. Zhou and G. Stell, Mol. Phys. **66**, 767 (1989).
- [15] A. K. Macpherson, Y. P. Carignan, and T. Vladimiroff, J. Chem. Phys. **87**, 1768 (1987).
- [16] S. T. Chui, Phys. Rev. B **43**, 11 523 (1990).
- [17] A. Gonzalez, J. A. White, F. L. Román, S. Velasco, and R. Evans, Phys. Rev. Lett. **79**, 2466 (1997); A. Gonzalez, J. A. White, F. L. Román, and R. Evans, J. Chem. Phys. **109**, 3637 (1998).
- [18] S. K. Nayak, P. Jena, K. D. Ball, and R. S. Berry, J. Chem. Phys. **108**, 234 (1998).
- [19] M. Schmidt, R. Kusche, B. von Issendorff, and H. Haberlandt, Nature (London) **393**, 238 (1998).
- [20] M. Robles, M. Lopez de Haro, A. Santos, and S. Bravo Yuste, J. Chem. Phys. **108**, 1290 (1998).
- [21] B. Doliwa and A. Heuer, Phys. Rev. Lett. **80**, 4915 (1998).
- [22] Z. Németh and H. Löwen, J. Phys.: Condens. Matter **10**, 6189 (1998).
- [23] W. S. Jodrey and E. M. Tory, Phys. Rev. A **32**, 2347 (1985).
- [24] I. Z. Fisher, *Statistical Theory of Liquids* (University of Chicago Press, Chicago, 1964).
- [25] J. L. Barrat and M. Klein, Annu. Rev. Phys. Chem. **42**, 23 (1991).
- [26] L. V. Woodcock and C. A. Angell, Phys. Rev. Lett. **47**, 1129 (1981).
- [27] W. Hoover and F. H. Ree, J. Chem. Phys. **49**, 3609 (1968).
- [28] H. Löwen, Phys. Rep. **237**, 249 (1994).
- [29] R. Bubeck, S. Naser, C. Bechinger, and P. Leiderer, Prog. Colloid Polym. Sci. **110**, 41 (1998).
- [30] A. K. Arora and B. V. R. Tata, Adv. Colloid Interface Sci. **78**, 49 (1998).
- [31] H. Löwen, J. P. Hansen, and J. N. Roux, Phys. Rev. A **44**, 1169 (1991).
- [32] Y. Rosenfeld, Phys. Rev. Lett. **63**, 980 (1989); Y. Rosenfeld, M. Schmidt, H. Löwen, and P. Tarazona, Phys. Rev. E **55**, 4245 (1996).